Universal Cybernetic Risk Framework: Closed-Loop Dynamic Stabilization of Systemic Contagion in Interconnected Financial Networks

Lanz C. W. J. Chan
Finamatrix Research Center, Singapore
Corresponding Author Email: lanz@finamatrix.net

Shin-Hung Pan
Department of Information Management
Chaoyang University of Technology, Taichung, Taiwan
Email: vincentpan@cyut.edu.tw

Wing-Keung Wong
Department of Finance, Fintech & Big Data Research Center,
Asia University, Taichung, Taiwan
Email: wong@asia.edu.tw

Published on September 30, 2026

Abstract

Modern financial markets operate as hyper-connected, non-linear dynamical networks where micro-level autonomous de-risking and algorithmic liquidation cascades generate catastrophic macro-prudential instabilities. Prevailing systemic risk frameworks—such as Value-at-Risk (VaR), Expected Shortfall (ES), and static DebtRank algorithms—function as open-loop, passive observational diagnostics that exhibit severe phase-lag errors during non-equilibrium liquidation spirals. This paper introduces the **Universal Cybernetic Risk Framework (UCRF)**, transforming systemic risk mitigation from an observational metric into an active, closed-loop control architecture tailored for Central Counterparty Clearinghouses (CCPs) and central bank emergency liquidity facilities. We formulate a fully coupled 3N-dimensional state-space dynamic model capturing the non-linear interplay among balance-sheet equity, unencumbered funding liquidity, and endogenous fire-sale price impacts. By treating bilateral default cascades as sector-bounded non-linearities within a Lur'e system formulation, we establish rigorous network stabilization criteria using Lur'e-Postnikov Lyapunov functions and Linear Matrix Inequalities (LMIs). Furthermore, we prove formal Input-to-State Stability (ISS), analytically deriving the compact invariant attractor bounds that guarantee bounded systemic drawdowns under worst-case exogenous shocks. Crucially, UCRF incorporates actuator saturation and finite interventional budget constraints, resolving the unrealistic assumption of unconstrained liquidity bailouts. Multi-node stress-testing under a dual-time-scale simulation framework demonstrates that UCRF dynamically arrests contagion propagation and curtails systemic drawdowns substantially more effectively than conventional macroprudential overlays and equal-budget uncoordinated interventions, establishing an operational, mathematically grounded paradigm for safeguarding interconnected financial systems.

Keywords: Systemic Risk; Closed-Loop Control Systems; Financial Networks; Lur'e Systems; Linear Matrix Inequalities (LMI); Input-to-State Stability (ISS); Liquidity Contagion; Fire Sales.

JEL Classifications: C61, C62, D85, G17, G28.

1. Introduction

The global financial architecture orchestrates the continuous intermediation of more than $500 trillion in gross nominal assets spanning commercial banking liabilities, over-the-counter (OTC) derivative networks, and automated exchange venues. In the wake of successive liquidity crises, global regulatory mandates such as Basel III/IV and Solvency II have sought to reinforce institutional resilience primarily through countercyclical capital buffers, static leverage constraints, and risk-weighted capital requirements. However, prevailing systemic risk paradigms—anchored predominantly in point-in-time observational statistics such as Value-at-Risk (VaR), Expected Shortfall (ES), and historical variance-covariance matrices—remain fundamentally reactive and *open-loop*. Because these classical measures presuppose return stationarity and distributional ergodicity, they inevitably exhibit destructive phase-lag errors during non-equilibrium tail events: they signal elevated systemic fragility only *after* cascade liquidations and structural balance-sheet impairments have already ignited self-reinforcing fire sales.

This structural vulnerability is acutely magnified by the structural transition toward sub-second algorithmic execution, decentralized Automated Market Making (AMM), and autonomous, agentic AI trading architectures. Recent empirical evidence underscores that the proliferation of digital assets and decentralized protocols introduces substantial time-varying connectedness and hidden shock transmission channels that bridge crypto liquidity pools with traditional equity markets (Sindhu et al., 2026). In contemporary interconnected capital markets, shock propagation occurs at temporal scales orders of magnitude faster than conventional regulatory intervention cycles. Financial systems operate as complex, adaptive networks characterized by severe macro-level externalities: rational, micro-level risk mitigation executed autonomously by a single distressed institution (e.g., rapid deleveraging, collateral recall, and margin buffering) directly drains unencumbered funding liquidity from adjacent counterparty nodes. This transmission generates dual, mutually reinforcing contagion channels: direct default spillovers across interbank obligation graphs, and indirect asset fire-sale cascades across common asset holdings (Brunnermeier & Pedersen, 2009; Cont & Schaanning, 2017). While pioneering network diagnostics—most notably Eisenberg-Noe clearing vectors and iterative DebtRank algorithms (Battiston et al., 2012; Eisenberg & Noe, 2001)—have significantly advanced the structural mapping of systemic fragility, they serve strictly as passive diagnostic tools. They lack real-time closed-loop actuation mechanisms capable of actively steering network state trajectories away from catastrophic collapse regimes.

To bridge this fundamental divide between structural diagnostic measurement and real-time stabilization, this paper introduces the **Universal Cybernetic Risk Framework (UCRF)**. Reconceptualizing systemic risk management through the rigorous principles of non-linear control engineering, information theory, and network dynamics, UCRF transforms macroprudential stabilization from an open-loop observational exercise into an active, continuous-time closed-loop control system. Crucially, UCRF is designed to be operationally embedded within systemic clearing infrastructures—specifically Central Counterparty Clearinghouses (CCPs) and central bank emergency lending facilities (Lender of Last Resort, LOLR). Rather than positing an idealized "frictionless stabilizer," the framework formally incorporates the physical realities of financial interventions: information acquisition latencies, actuator saturation, and

strictly finite emergency liquidity budgets.

Key Contributions of this Paper:

1. **Coupled 3N-Dimensional State-Space Network Modeling:** This study constructs a rigorous, continuous-time dynamic state-space framework of an interconnected financial network where each node's state is explicitly governed by three coupled, non-linear dimensions: net balance-sheet equity capital, unencumbered funding liquidity, and real-time mark-to-market asset price impacts. This restores balance-sheet accounting conservation and captures direct counterparty default contagion alongside indirect, market-microstructure-driven fire-sale dynamics.

2. **Lur'e System Formulation and Linear Matrix Inequality (LMI) Solvability:** This study formalizes the non-linear, discontinuous threshold dynamics of institutional insolvency as sector-bounded non-linearities. By recasting the entire closed-loop financial network as an interconnected **Lur'e dynamical system**, we prove that network stabilization can be systematically synthesized using parameterized **Lur'e-Postnikov Lyapunov functions** and solved globally via convex **Linear Matrix Inequalities (LMIs)**.

3. **Input-to-State Stability (ISS) under Bounded Tail Shocks:** Moving beyond local asymptotic linearization, this study mathematically proves that the closed-loop financial network under UCRF satisfies strict **Input-to-State Stability (ISS)** criteria. We analytically derive the explicit bounds of the compact invariant attractor set, proving that for any arbitrarily bounded exogenous macroeconomic shock, systemic network drawdowns remain strictly contained within a provably stable boundary layer.

4. **Budget-Constrained Actuation and Dual-Time-Scale Validation:** This study explicitly incorporate actuator saturation and statutory central bank liquidity budget ceilings into the feedback control law, eliminating the economically unviable assumption of unbounded capital injections. Using extensive stress tests on heterogeneous scale-free networks under a dual-time-scale architecture (sub-second margin/circuit-breaker throttling coupled with multi-minute liquidity facility actuation), we demonstrate that UCRF significantly outperforms both conventional static capital buffers and equal-budget uncoordinated bailouts.

The remainder of this paper is structured as follows: Section 2 reviews foundational literature in balance-sheet contagion, fire-sale mechanisms, and dynamic control theory. Section 3 constructs the mathematical architecture and coupled state-space equations of the UCRF. Section 4 provides formal non-linear stability proofs, deriving LMI conditions and ISS invariant bounds. Section 5 details the simulation methodology, experimental benchmarks, and empirical stress-testing results. Section 6 addresses practical implementation constraints, including state observability and latency dynamics. Section 7 concludes.

2. Literature Review

The theoretical foundation of systemic risk mitigation in hyper-connected financial networks rests at the intersection of three mature yet historically disjoint literatures: (i) structural balance-sheet default contagion, (ii) endogenous market microstructure and fire-sale liquidity spirals, and (iii) dynamic cybernetic control systems.

2.1 Direct Balance-Sheet Contagion and Network Topology

Structural modeling of direct interbank contagion originated with the deterministic clearing payment framework of Eisenberg and Noe (2001), which established the existence and uniqueness of clearing vectors under simultaneous obligations. Subsequent research demonstrated that financial networks possess a fundamental "robust-yet-fragile" topology (Gai & Kapadia, 2010): high interbank connectivity dissipates localized shocks during benign regimes, but acts as a rapid conduit of systemic cascade collapse once shock magnitudes breach institutional capital cushions. Crucially, empirical investigations have revealed that these structural contagion vulnerabilities are profoundly compounded by cross-border trade linkages and real-economic interdependencies, where bilateral commercial integration substantially accelerates the velocity and geographic reach of cross-country shock transmission (Khan et al., 2005). In modern financial ecosystems, these fundamental exposures map into complex bilateral liability graphs that operate as primary transmission channels for non-equilibrium liquidity drains.

Historically, researchers recognized that financial crisis transmission exhibits characteristics akin to physical field dynamics, where systemic spillovers operate not merely through deterministic balance-sheet links, but through dynamic 'inductance' feedback loops across sovereign and banking counterparties (Wan & Wong, 2001). This dynamic conceptualization prefigured modern recursive algorithms such as DebtRank (Battiston et al., 2012) developed *DebtRank*, an axiomatic recursive algorithm demonstrating that equity devaluations induce continuous feedback distress cycles across counterparty chains. Recent extensions have enriched this topological paradigm by incorporating higher-order tensor structures, multilayer derivative dependency graphs, and capacity-constrained flow networks (Huang et al., 2025; Montañez Jacquez et al. 2026). Nevertheless, these structural network frameworks remain predominantly *discrete-time diagnostic formulations*. They provide post-facto metrics of topological centrality (e.g., eigenvector centrality, DebtRank impact scores) but lack continuous-time dynamic state representations capable of synthesizing automated stabilizing control laws.

2.2 Indirect Contagion, Fire Sales, and Liquidity Spirals

A critical limitation of pure interbank obligation graphs is their omission of indirect, market-mediated contagion. Landmark work by Cifuentes et al. (2005) revealed that regulatory minimum capital constraints force distressed institutions into non-cooperative asset liquidations, depressing mark-to-market prices and inflicting balance-sheet write-downs on non-defaulting third parties holding overlapping portfolios.

This endogenous vulnerability was formalized by Brunnermeier and Pedersen (2009), who articulated the self-reinforcing interaction between *funding liquidity* (traders' capital availability) and *market liquidity* (asset market depth). Under adverse stress, capital losses trigger collateral hair-cut escalations and margin

calls ("margin spirals"), which induce forced liquidations and illiquidity discounts ("loss spirals"). Further empirical and theoretical formalizations by Cont and Schaanning (2017) and Greenwood et al. (2015) proved that in modern multi-trillion-dollar asset markets, indirect fire-sale spillovers frequently exceed direct counterparty default losses by an order of magnitude. Microstructural pricing parameters—such as Kyle's price impact λ (Kyle, 1985) and Amihud's illiquidity ratio (Amihud, 2002)—govern the velocity of this fire-sale feedback. Despite these critical insights, macroprudential capital regulations (e.g., countercyclical capital buffers under Basel III/IV) continue to operate on quarterly bureaucratic supervisory cycles, failing to match the millisecond-to-minute velocity of liquidity-drain dynamics.

2.3 Cybernetics, Networked Control Systems, and the Research Gap

Concurrently, cybernetics—the science of communication, feedback, and dynamic control in complex systems (Ashby, 1956; Wiener, 1948)—has evolved into sophisticated mathematical frameworks for networked dynamic stabilization. In economics and algorithmic trading, cybernetic feedback loops have been implemented for high-frequency volatility damping and portfolio drawdown control (Chan & Wong, 2012; Hansen & Sargent, 2008). In complex physical infrastructures (e.g., smart power grids, distributed transport networks), non-linear cascade failures are prevented by synthesizing state-dependent Lyapunov controllers and solving convex Linear Matrix Inequalities (LMIs) that guarantee global asymptotic stability (Boyd et al., 1994; Khalil, 2002). In algorithmic trading and quantitative execution, preliminary frameworks established the viability of automated feedback rules through dedicated risk-cybernetics protocols designed to dynamically curtail portfolio tail risk (Chan & Wong, 2012, 2018). However, extending these principles from isolated execution venues to systemic multi-agent banking networks with counterparty externalities requires an entirely new mathematical formulation.

More specifically, dynamic multi-agent systems featuring discontinuous saturation or threshold dynamics are mathematically encapsulated through **Lur'e systems**—interconnections of linear dynamical subsystems with memoryless, sector-bounded non-linear feedback operators (Lur'e & Postnikov, 1944). While Lur'e formulations and Input-to-State Stability (ISS) paradigms (Sontag, 1989) are ubiquitous in engineering cascade mitigation, their rigorous application to financial systemic risk networks remains an unaddressed frontier.

The Identified Research Gap:

The existing body of literature presents a persistent dichotomy:

(1) *Financial network models* capture realistic balance-sheet contagion and fire-sale spirals, but remain observational, static, and open-loop.

(2) *Control-theoretic frameworks* offer formal stability proofs and real-time stabilization algorithms, but have not incorporated the structural realities of interbank balance sheets, mark-to-market liquidation elasticities, and finite central bank liquidity constraints.

The **Universal Cybernetic Risk Framework (UCRF)** bridges this divide. By transforming the coupled non-linear equations of interbank default and fire-sale contagion into a unified Lur'e-type networked control system, UCRF provides the first mathematically closed-loop, budget-constrained stabilization architecture capable of actively extinguishing systemic contagion cascades in real time.

3. Mathematical Architecture of the UCRF

3.1 Network Topology and Composite State-Space Representation

Consider a financial network formalized as a directed, weighted graph G=(V,E,**W**), where V={1,2,…,*N*} represents *N* systemically interconnected institutions (e.g., commercial banks, broker-dealers, clearing members) and $E \subseteq V \times V$ denotes bilateral contractual exposures. The matrix $\boldsymbol{W} = [W_{ij}] \in \mathbb{R}_{+}^{N \times N}$ defines gross bilateral liabilities, where $W_{ji} \geq 0$ represents the uncollateralized nominal liability owed by institution *j* to institution *i*.

The physical balance sheet and market condition of node *i* at continuous time $t \geq 0$ is governed by a local state vector $x_i(t) = [e_i(t), l_i(t), p_i(t)]^T \in \mathbb{R}^3$, defined as:

- $e_i(t) \in \mathbb{R}$: Net Tier-1 equity capital buffer (solvency margin above regulatory insolvency, where $e_i < 0$ denotes nominal default).
- $l_i(t) \in \mathbb{R}_+$: Unencumbered, high-quality funding liquidity reserve available for immediate settlement.
- $p_i(t) \in \mathbb{R}_+$: Real-time mark-to-market price index of node *i* 's core marketable asset holdings.

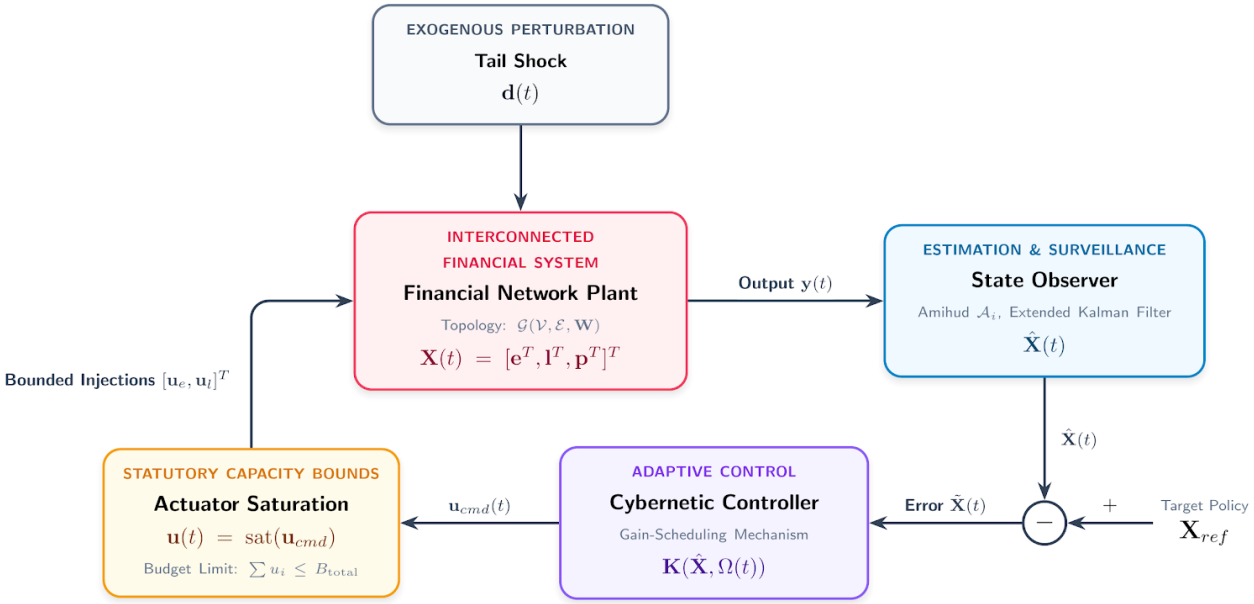
To ensure algebraic consistency, we assemble the global network state by grouping the state vectors into partitioned macro-variables:

$$\mathbf{X}(t) = \begin{bmatrix} \mathbf{e}(t) \\ \mathbf{l}(t) \\ \mathbf{p}(t) \end{bmatrix} \in \mathbb{R}^{3N}, \qquad where\ \mathbf{e}(t), \mathbf{l}(t), \mathbf{p}(t) \in \mathbb{R}^{N}.$$

The global control actuation vector is partitioned as $\mathbf{u}(t) = [\mathbf{u}_e(t)^T, \mathbf{u}_l(t)^T]^T \in \mathbb{R}^{2N}$, representing targeted capital injections and emergency central bank liquidity accommodations, respectively. Exogenous macroeconomic and credit disturbances are collected in $\mathbf{d}(t) = [\mathbf{d}_e(t)^T, \mathbf{d}_l(t)^T, \mathbf{d}_p(t)^T]^T \in \mathbb{R}^{3N}$.

To operationalize real-time macroprudential stabilization, the dynamic interactions between the interbank ecosystem, regulatory monitoring, and intervention mechanisms are structured into the closed-loop cybernetic feedback architecture depicted in Figure 1.

Figure 1: Architectural Schematic of the Universal Cybernetic Risk Framework (UCRF)



Note: The closed-loop control system formalizes macroprudential stabilization across an interconnected financial network. An exogenous tail disturbance $\mathrm{d}(t)$ perturbs the $3N$-dimensional financial network plant (governed by coupled equity capital, funding liquidity, and asset price dynamics). The monitoring infrastructure extracts noisy market observations $\mathrm{y}(t)$ and empirical illiquidity signals $\mathrm{A}(t)$, which a dynamic state observer reconstructs into estimated network states $\hat{\mathrm{X}}(t)$. The cybernetic controller computes the error state $\tilde{\mathrm{X}}(t) = \hat{\mathrm{X}}(t) - \mathrm{X}_{ref}$ and synthesizes the commanded feedback policy $\mathrm{u}_{cmd}(t) = -\mathrm{K}(\hat{\mathrm{X}})\tilde{\mathrm{X}}(t)$ via dynamic gain-scheduling parameterized by the topological distress index $\Omega(t)$. Before actuation, the signal passes through an Actuator Saturation & Budgetary Constraint Operator enforcing component-wise physical limits U_{max} and the aggregate central bank liquidity budget ceiling B_{total}, delivering bounded capital relief $\mathrm{u}_e(t)$ and emergency liquidity $\mathrm{u}_l(t)$ to arrest contagion cascades in real time.

The framework operates through four interconnected operational subsystems:

(1) The Interconnected Financial Plant:

The central plant consists of N heterogeneous financial institutions interconnected via bilateral liability graphs W and overlapping marketable asset holdings. The unforced plant dynamics inherently exhibit two non-linear amplification loops: direct balance-sheet default transmission (activated when $e_i < 0$) and market-mediated fire-sale spirals driven by price devaluations $\dot{p}_i(t)$. Exogenous tail-risk shocks $\mathrm{d}(t) = [\mathrm{d}_e^T, \mathrm{d}_l^T, \mathrm{d}_p^T]^T$ inject sudden stress into capital reserves, wholesale funding channels, and asset valuations.

(2) Monitoring Infrastructure and Dynamic State Estimation:

Because bilateral Over-the-Counter (OTC) obligations and unencumbered funding liquidity reserves $\mathrm{l}(t)$ cannot be observed synchronously across all market participants, the monitoring sensor array collects public market output vectors $\mathrm{y}(t)$ alongside continuous microstructure depth metrics—specifically the Amihud illiquidity estimator $\mathrm{A}_i(t)$. A dynamic Luenberger-type state observer reconstructs the latent network state $\hat{\mathrm{X}}(t) = [\hat{\mathrm{e}}^T, \hat{\mathrm{l}}^T, \hat{\mathrm{p}}^T]^T$, filtering high-frequency noise from structural liquidity drains.

(3) Cybernetic Gain-Scheduling Controller:

The reconstructed state is continuously benchmarked against the target macroprudential equilibrium X_{ref}, generating the network error signal $\widetilde{\mathrm{X}}(t) = \widehat{\mathrm{X}}(t) - \mathrm{X}_{ref}$. The cybernetic controller dynamically scales its multi-variable block gain matrix $\mathrm{K}(\widehat{\mathrm{X}})$ according to the systemic network distress index $\Omega(t)$. This ensures that control gains remain small during benign regimes to prevent market distortions, but amplify exponentially when counterparty distress clusters around critical topological hubs.

(4) Actuator Saturation and Statutory Budgetary Enforcement:

Crucially, commanded control policies $\mathrm{u}_{cmd}(t)$ are not fed directly into the interbank plant as unconstrained capital. Instead, signals pass through a hard non-linear saturation operator, $\mathrm{u}(t) = \mathrm{sat}(\mathrm{u}_{cmd}(t))$. This actuator module imposes component-wise operational capacity caps $(U_{e,i}^{max}, U_{l,i}^{max})$ representing practical clearing facility throughputs, alongside an aggregate fiscal conservation constraint: $\sum_{i=1}^{N}(u_{e,i}(t) + u_{l,i}(t)) \leq B_{total}(t)$. This ensures that emergency discount-window liquidity $\mathrm{u}_l(t)$ and supervisory capital forbearance $\mathrm{u}_e(t)$ strictly adhere to central bank statutory budget limits.

3.2 Uncontrolled Cascade Dynamics

In the absence of closed-loop regulatory intervention ($\mathbf{u}(t) \equiv \mathbf{0}$), shock propagation is driven by the coupled dynamics of direct interbank obligation default and indirect, market-mediated fire sales:

$$\frac{de_i(t)}{dt} = -\gamma_i e_i(t) - \sum_{j=1}^{N} C_{ji}\,\Phi\left(e_j(t)\right) + q_i \cdot \frac{dp_i(t)}{dt} + d_{e,i}(t), \tag{1}$$

$$\frac{dl_i(t)}{dt} = -k_i\left(l_i(t) - l_{ref,i}\right) - \sum_{j=1}^{N} \Theta_{ji}\, I_{\{e_j(t)<0\}} - \beta_i\left[-\frac{dp_i(t)}{dt}\right]^{+} + d_{l,i}(t),$$

$$\frac{dp_i(t)}{dt} = -\Lambda_i(t) \sum_{k=1}^{N} \mathrm{S}_k\left(e_k(t), l_k(t)\right) + d_{p,i}(t).$$

Where the structural parameters and functional operators are defined as follows:

(1) **Insolvency Contagion Operator (Φ):**

The term $\Phi(\mathrm{e_j(t)}) = \max(0, -\mathrm{e_j(t)}) \geq 0$ captures the unrecovered insolvency shortfall of counterparty j. The exposure coupling coefficient is defined as $C_{ij} = \frac{W_{ji}}{\sum_{k=1}^{N} W_{jk}}$, denoting the fraction of j's total default obligations absorbed by node i. The strictly negative sign ($-\sum \mathrm{C_{ji}}\Phi$) guarantees that counterparty insolvency depletes, rather than subsidizes, node i's equity.

(2) **Mark-to-Market Balance-Sheet Feedback:**

$q_i > 0$ represents the portfolio volume of the marketable asset held by institution i. When asset prices deteriorate ($d_{pi}/d_t < 0$), the product $+q_i \frac{dp_i}{dt}$ directly reduces capital buffer growth through mark-to-market balance-sheet write-downs.

(3) **Liquidity Run and Margin Call Dynamics:**

$\kappa_i > 0$ represents the structural rate of cash-flow restoration toward target operating liquidity $l_{ref,i}$. The coefficient $\Theta_{ji} \geq 0$ models interbank wholesale funding runs, where the discrete indicator $I_{\{ej(t)<0\}}$ abruptly halts rollover credit upon counterparty default. The parameter $\beta_i \geq 0$ dictates variation margin call elasticities triggered by downward asset price shocks ($[x]^+=\max(0, x)$).

(4) **Endogenous Fire-Sale Price Impact and Microstructure Estimator:**

$S_k(e_k, l_k) = \mu_e \max(0, \bar{e}_k - e_k) + \mu_l \max(0, \bar{l}_k - l_k) \geq 0$ represents forced distress liquidations executed when capital or funding reserves breach supervisory thresholds $\bar{e}_k, \bar{l}_k$.

To ground market depth in empirical microstructure (replacing speculative technical analysis formulations), the dynamic illiquidity coefficient $\Lambda_i(t)$is parameterized using the **Amihud Illiquidity Estimator** $A_i(t)$:

$$\Lambda_i(t) = \Lambda_{0,i} \cdot \big(1 + \omega_i A_i(t)\big), \qquad A_i(t) = \frac{|\Delta p_i(t)|}{V_{total,i}(t) \cdot p_i(t)}, \tag{2}$$

where $\Lambda_{0,i}$ is baseline Kyle price impact depth, $V_{total,i}(t)$ is trading volume, and $\omega_i > 0$ calibrates market depth degradation during liquidity panics.

3.3 Closed-Loop Cybernetic Control Architecture

To arrest contagion without asserting unbounded public fiscal interventions, UCRF formalizes the stabilization problem through bounded, state-dependent closed-loop feedback.

Define the state tracking error relative to target prudential equilibrium $\mathbf{X}_{ref} = \left[\boldsymbol{e}_{ref}^T, \boldsymbol{l}_{ref}^T, \boldsymbol{p}_{ref}^T\right]^T$ as:

$$\widetilde{\mathbf{X}}(t) = \mathbf{X}(t) - \mathbf{X}_{ref} \in \mathbb{R}^{3N}. \tag{3}$$

The aggregate non-linear error dynamics of the network can be assembled into standard matrix state-space form:

$$\frac{d\widetilde{\mathbf{X}}(t)}{dt} = \mathbf{A}\widetilde{\mathbf{X}}(t) - \mathbf{B}_{\Phi}\boldsymbol{\Phi}\big(\mathbf{e}(t)\big) + \mathbf{B}\mathbf{u}(t) + \mathbf{D}\mathbf{d}(t), \tag{4}$$

where:

- $\mathbf{A} = \text{blkdiag}(-\mathbf{\Gamma}, -\mathbf{K}_\text{l}, -\mathbf{\Lambda}_0) \in \mathbb{R}^{3N\times 3N}$ represents nominal open-loop dissipation ($\mathbf{\Gamma}$=diag(γ_i), $\mathbf{K}_\text{l}$=diag(κ_i)).
- $\mathbf{\Phi}\big(\mathbf{e}(t)\big) = \big[\Phi\big(\text{e}_1(t)\big), \dots, \Phi\big(\text{e}_N(t)\big)\big]^T \in \mathbb{R}^N$ collects the non-linear default transmission operators.
- $\mathbf{B}_\Phi = \begin{bmatrix} C^T \\ 0_{N\times N} \\ 0_{N\times N} \end{bmatrix} \in \mathbb{R}^{3N\times N}$, with $\mathbf{C} = [C_{ij}] \in \mathbb{R}_+^{N\times N}$.
- $\mathbf{B} = \begin{bmatrix} \mathbf{I}_\text{N} & 0_{N\times N} \\ 0_{N\times N} & \mathbf{I}_\text{N} \\ 0_{N\times N} & 0_{N\times N} \end{bmatrix} \in \mathbb{R}^{3N\times 2N}$ is the input distribution matrix mapping control inputs $\mathbf{u} = [\mathbf{u}_e^T, \mathbf{u}_l^T]^T$ directly into capital and liquidity state derivatives.
- $\mathbf{D}$=$\mathbf{I}_{3N}$ maps exogenous shock vectors.

Dynamic Gain-Scheduling Control Policy

The commanded regulatory actuation $\mathbf{u}_{cmd}(t) \in \mathbb{R}^{2N}$ is governed by a dimensionally consistent, state-dependent block gain matrix:

$$\mathbf{u}_{cmd}(t) = -\mathbf{K}\big(\widetilde{\mathbf{X}}\big)\widetilde{\mathbf{X}}(t) = -\begin{bmatrix} \mathbf{K}_{ee}\big(\widetilde{\mathbf{X}}\big) & \mathbf{K}_{el}\big(\widetilde{\mathbf{X}}\big) & \mathbf{K}_{ep}\big(\widetilde{\mathbf{X}}\big) \\ \mathbf{K}_{le}\big(\widetilde{\mathbf{X}}\big) & \mathbf{K}_{ll}\big(\widetilde{\mathbf{X}}\big) & \mathbf{K}_{lp}\big(\widetilde{\mathbf{X}}\big) \end{bmatrix} \begin{bmatrix} \tilde{\mathbf{e}}(t) \\ \tilde{\mathbf{l}}(t) \\ \tilde{\mathbf{p}}(t) \end{bmatrix}. \tag{5}$$

Each diagonal block $\mathbf{K}_{\alpha\beta}(\widetilde{\mathbf{X}}) \in \mathbb{R}^{N\times N}$ is dynamically scheduled via the real-time systemic network distress index Ω(t):

$$\mathbf{K}_{ee}\big(\widetilde{\mathbf{X}}\big) = \mathbf{K}_{0,ee} + \lambda \cdot diag\left(e^{\Omega(\text{t})}A_1(t), \dots, e^{\Omega(\text{t})}A_N(t)\right), \tag{6}$$

$$\Omega(\text{t}) = \sum_{i=1}^{N}\sum_{j=1}^{N} C_{ji}\frac{\left|e_j(t) - e_j(0)\right|}{e_j(0)}. \tag{7}$$

Actuator Saturation and Statutory Budget Constraints

To resolve the "infinite bailout / money-printer" fallacy, the realized control vector **u**(*t*) is subjected to strict **component-wise saturation** and **aggregate budget conservation**:

$$\mathbf{u}(t) = \text{sat}\big(\mathbf{u}_{cmd}(t)\big),$$

$$subject\ to: \begin{cases} 0 \le u_{e,i}(t) \le U_{e,i}^{max}, & \forall_i \in \{1, \dots, N\} \\ 0 \le u_{l,i}(t) \le U_{l,i}^{max}, & \forall_i \in \{1, \dots, N\} \\ \sum_{i=1}^{N} \left(u_{e,i}(t) + u_{l,i}(t)\right) \le B_{total}(t) \end{cases}, \tag{8}$$

where $B_{total}(t)$ denotes the finite, statutory emergency capacity of the central bank's discount facility or resolution fund.

4. Stability Analysis and Theoretical Results

To establish rigorous mathematical guarantees for the Universal Cybernetic Risk Framework (UCRF), this section reformulates the closed-loop financial network as an interconnected **Lur'e dynamical system**. We prove that despite discontinuous, non-linear balance-sheet default thresholds and fire-sale price feedback, the network achieves global asymptotic stability under nominal conditions and strict **Input-to-State Stability (ISS)** under bounded macroeconomic stress shocks.

4.1 Lur'e System Formulation and Sector-Bounded Non-linearities

Subtracting the prudential target equilibrium $\mathbf{X}_{ref}$ from the dynamic equations established in Section 3, the closed-loop tracking error dynamics $\widetilde{\mathbf{X}}(t) = \mathbf{X}(t) - \mathbf{X}_{ref} \in \mathrm{R}^{3N}$ are expressed as:

$$\frac{d\widetilde{\mathbf{X}}(t)}{dt} = \mathbf{A}_{cl}\widetilde{\mathbf{X}}(t) - \mathbf{B}_{\Phi}\mathbf{\Phi}\left(\tilde{\mathbf{e}}(t)\right) + \mathbf{D}\mathbf{d}(t), \tag{9}$$

where $\mathbf{A}_{cl} = \mathbf{A} - \mathbf{B}\mathbf{K}_0 \in \mathrm{R}^{3N\times 3N}$ represents the nominal closed-loop Hurwitz state matrix, and $\mathbf{\Phi}(\tilde{\mathbf{e}}(t)) = [\Phi(\tilde{e}_1), \dots, \Phi(\tilde{e}_N)]^T \in \mathrm{R}^N$ collects the decentralized counterparty insolvency operators.

Lemma 1 (Sector Characterization of Default Transmission):

For each node $j \in \{1, \dots, N\}$, the insolvency shortfall function $\Phi(e_j) = max\ (0, -e_j)$ relative to a non-negative reference capital buffer $e_{ref,j} \ge 0$ satisfies a decentralized sector condition within $[0, k_\phi]$ with $k_\phi = 1$:

$$\Phi\left(\tilde{e}_j(t)\right) \cdot \left[\Phi\left(\tilde{e}_j(t)\right) + \tilde{e}_j(t)\right] \le 0, \qquad \forall \tilde{e}_j(t) \in \mathbb{R}. \tag{10}$$

Proof:

If $e_j(t) \ge 0$, then $\Phi(e_j) = 0$, and the inequality holds trivially ($0 \le 0$). If $e_j(t) < 0$, then $\Phi(e_j) = -e_j > 0$. Since $\tilde{e}_j = e_j - e_{ref,j} \le e_j < 0$, we have $\Phi(e_j) + \tilde{e}_j \le -e_j + e_j = 0$.

Aggregating across all N institutions, the network-wide non-linearity satisfies the multi-variable sector

inequality:

$$\boldsymbol{\Phi}(\tilde{\boldsymbol{e}})^{T}\boldsymbol{\Lambda}\left(\boldsymbol{\Phi}(\tilde{\boldsymbol{e}})+\mathbf{H}\widetilde{\mathbf{X}}\right)\leq 0, \tag{11}$$

for any diagonal positive semi-definite multiplier matrix $\boldsymbol{\Lambda}=\mathrm{diag}(\lambda_1,\ldots,\lambda_N)\geq 0$, where $\mathbf{H}=[\mathbf{I}_N,\mathbf{0}_{N\times N},\mathbf{0}_{N\times N}]\in \mathrm{R}^{N\times 3N}$ is the selection matrix extracting capital error states $\tilde{\mathbf{e}}=\mathbf{H}\widetilde{\mathbf{X}}$.

4.2 Asymptotic Stability via Linear Matrix Inequalities (LMIs)

We first evaluate the nominal autonomous system in the absence of exogenous shocks ($\mathbf{d}(t)\equiv\mathbf{0}$).

Theorem 1 (Absolute Stability of the Cybernetic Closed-Loop Network):

Consider the autonomous closed-loop financial network $\dot{\widetilde{\mathbf{X}}}=\mathbf{A}_{cl}\widetilde{\mathbf{X}}-\mathbf{B}_{\Phi}\boldsymbol{\Phi}(\tilde{\mathbf{e}})$. The equilibrium state $\widetilde{\mathbf{X}}=\mathbf{0}$ is globally asymptotically stable (GAS) if there exist a symmetric positive-definite matrix $\mathbf{P}=\mathbf{P}^{T}>0\in \mathrm{R}^{3N\times 3N}$ and a diagonal non-negative multiplier matrix $\boldsymbol{\Lambda}=\mathrm{diag}(\lambda_1,\ldots,\lambda_N)\geq 0$ such that the following **Linear Matrix Inequality (LMI)** is satisfied:

$$\begin{bmatrix}\mathbf{A}_{\mathrm{cl}}^{\mathrm{T}}\mathbf{P}+\mathbf{P}\mathbf{A}_{\mathrm{cl}} & -\mathbf{P}\mathbf{B}_{\boldsymbol{\Phi}}-\frac{1}{2}\mathbf{H}^{\mathrm{T}}\boldsymbol{\Lambda}\\ -\mathbf{B}_{\Phi}^{\mathrm{T}}\mathbf{P}-\frac{1}{2}\boldsymbol{\Lambda}\mathbf{H} & -\boldsymbol{\Lambda}\end{bmatrix}<0. \tag{12}$$

Proof:

Construct the quadratic Lur'e-Postnikov Lyapunov candidate function:

$$V(\widetilde{\mathbf{X}})=\widetilde{\mathbf{X}}^{T}\mathbf{P}\widetilde{\mathbf{X}},\ \mathbf{P}=\mathbf{P}^{T}>0.$$

$V(\widetilde{\mathbf{X}})$ is radially unbounded since $\lambda_{min}(\mathbf{P})\parallel\widetilde{\mathbf{X}}\parallel^{2}\leq V(\widetilde{\mathbf{X}})\leq\lambda_{max}(\mathbf{P})\parallel\widetilde{\mathbf{X}}\parallel^{2}$. Taking the continuous-time derivative of $V(\widetilde{\mathbf{X}})$ along the nominal trajectories yields:

$$\dot{V}(\widetilde{\mathbf{X}})=\dot{\widetilde{\mathbf{X}}}^{T}\mathbf{P}\widetilde{\mathbf{X}}+\widetilde{\mathbf{X}}^{T}\mathbf{P}\dot{\widetilde{\mathbf{X}}}=\widetilde{\mathbf{X}}^{T}\left(\mathbf{A}_{cl}^{T}\mathbf{P}+\mathbf{P}\mathbf{A}_{cl}\right)\widetilde{\mathbf{X}}-2\widetilde{\mathbf{X}}^{T}\mathbf{P}\mathbf{B}_{\Phi}\boldsymbol{\Phi}(\tilde{\mathbf{e}}).$$

By applying the **S-procedure** (Boyd et al., 1994), $\dot{V}(\widetilde{\mathbf{X}})<0$ holds for all non-zero states $\widetilde{\mathbf{X}}\neq\mathbf{0}$ if there exists $\boldsymbol{\Lambda}\geq 0$ such that:

$$S(\widetilde{\mathbf{X}},\boldsymbol{\Phi})=\dot{V}(\widetilde{\mathbf{X}})-2\boldsymbol{\Phi}(\tilde{\boldsymbol{e}})^{T}\boldsymbol{\Lambda}\left(\boldsymbol{\Phi}(\tilde{\boldsymbol{e}})+\mathbf{H}\widetilde{\mathbf{X}}\right)<\mathbf{0}.$$

Expanding and expressing $S(\widetilde{\mathbf{X}},\boldsymbol{\Phi})$ in quadratic form over the augmented state vector $\boldsymbol{\xi}=[\widetilde{\mathbf{X}}^{T},\boldsymbol{\Phi}^{T}]^{T}$:

$$S(\widetilde{\mathbf{X}}, \boldsymbol{\Phi}) = \begin{bmatrix} \widetilde{\mathbf{X}} \\ \boldsymbol{\Phi} \end{bmatrix}^T \begin{bmatrix} \mathbf{A}_{\mathrm{cl}}^{\mathrm{T}}\mathbf{P} + \mathbf{P}\mathbf{A}_{\mathrm{cl}} & -\mathbf{P}\mathbf{B}_{\boldsymbol{\Phi}} - \frac{1}{2}\mathbf{H}^{\mathrm{T}}\boldsymbol{\Lambda} \\ -\mathbf{B}_{\Phi}^{\mathrm{T}}\mathbf{P} - \frac{1}{2}\boldsymbol{\Lambda}\mathbf{H} & -\boldsymbol{\Lambda} \end{bmatrix} \begin{bmatrix} \widetilde{\mathbf{X}} \\ \boldsymbol{\Phi} \end{bmatrix} < 0.$$

If the block LMI is strictly negative definite, then $\dot{V}(\widetilde{\mathbf{X}}) \leq -\alpha \parallel \widetilde{\mathbf{X}} \parallel^2$ for some $\alpha > 0$. By Lyapunov's direct method, the origin $\widetilde{\mathbf{X}} = \mathbf{0}$ is globally asymptotically stable, guaranteeing that cascading defaults are structurally incapable of sustaining self-amplifying growth.

4.3 Input-to-State Stability (ISS) under Bounded Tail Shocks

In realistic market environments, the financial network is continuously subjected to persistent exogenous tail shocks $\mathbf{d}(t) \neq \mathbf{0}$.

In realistic market environments, the financial network is continuously subjected to persistent, multi-frequency exogenous tail shocks d(t) ≠ 0. Severe geopolitical and macroeconomic crises frequently generate high-frequency volatility spillovers that cross commodity and capital markets simultaneously (Suissi & Mroua, 2026), necessitating formal Input-to-State Stability (ISS) guarantees.

Theorem 2 (Input-to-State Stability and Invariant Attractor Bounds):

Assume the LMI in Theorem 1 is satisfied such that $\mathbf{Q} = -(\mathbf{A}_{\mathrm{cl}}^{\mathrm{T}}\mathbf{P} + \mathbf{P}\mathbf{A}_{\mathrm{cl}}) > 0$. If exogenous macroeconomic disturbances are uniformly bounded in Euclidean norm such that $sup_{t\geq 0}\|d(t)\| \leq d_{max} < \infty$, then the closed-loop system is **Input-to-State Stable (ISS)**. Furthermore, the network state error $\widetilde{\mathbf{X}}(t)$ asymptotically converges to a compact invariant attractor set B_{δ}:

$$B_{\delta} = \left\{\widetilde{\mathbf{X}} \in R^{3N} : \left\|\widetilde{\mathbf{X}}\right\| \leq \delta\right\}, where\ \delta = \frac{2\lambda_{max}(\mathbf{P})\|\mathbf{D}\|d_{max}}{\lambda_{min}(\mathbf{Q})\sqrt{\frac{\lambda_{min}(\mathbf{P})}{\lambda_{max}(\mathbf{P})}}}. \quad (13)$$

Proof:

Evaluating the time derivative of $V(\widetilde{\mathbf{X}}) = \widetilde{\mathbf{X}}^T\mathbf{P}\widetilde{\mathbf{X}}$ along the disturbed trajectories $\dot{\widetilde{\mathbf{X}}} = \mathbf{A}_{cl}\widetilde{\mathbf{X}} - \mathbf{B}_{\Phi}\boldsymbol{\Phi} + \mathbf{D}\mathbf{d}$:

$$\dot{V}(\widetilde{\mathbf{X}}) = \widetilde{\mathbf{X}}^T\left(\mathbf{A}_{cl}^T\mathbf{P} + \mathbf{P}\mathbf{A}_{cl}\right)\widetilde{\mathbf{X}} - 2\widetilde{\mathbf{X}}^T\mathbf{P}\mathbf{B}_{\Phi}\boldsymbol{\Phi} + 2\widetilde{\mathbf{X}}^T\mathbf{P}\mathbf{D}\mathbf{d}(t).$$

Substituting the negative-definiteness established via the S-procedure in Theorem 1:

$$\dot{V}(\widetilde{\mathbf{X}}) \leq -\lambda_{min}(\mathbf{Q}) \parallel \widetilde{\mathbf{X}} \parallel^2 + 2 \parallel \widetilde{\mathbf{X}} \parallel \parallel \mathbf{P}\mathbf{D} \parallel d_{max}.$$

Decomposing the quadratic dissipation term into two halves:

$$\dot{V}(\widetilde{\mathbf{X}}) \leq -\frac{1}{2}\lambda_{min}(\mathbf{Q}) \parallel \widetilde{\mathbf{X}} \parallel^{2} - \frac{1}{2}\lambda_{min}(\mathbf{Q}) \parallel \widetilde{\mathbf{X}} \parallel^{2} + 2 \parallel \widetilde{\mathbf{X}} \parallel \parallel \mathbf{PD} \parallel d_{max}.$$

The second half satisfies $-\frac{1}{2}\lambda_{min}(\mathbf{Q}) \parallel \widetilde{\mathbf{X}} \parallel^{2} + 2 \parallel \widetilde{\mathbf{X}} \parallel \parallel \mathbf{PD} \parallel d_{max} \leq 0$ whenever the state norm satisfies:

$$\parallel \widetilde{\mathbf{X}}(t) \parallel \geq \frac{4 \parallel \mathbf{PD} \parallel d_{max}}{\lambda_{min}(\mathbf{Q})} \equiv \mu.$$

Consequently, for all $\parallel \widetilde{\mathbf{X}} \parallel \geq \mu$, we have:

$$\dot{V}(\widetilde{\mathbf{X}}) \leq -\frac{1}{2}\lambda_{min}(\mathbf{Q}) \parallel \widetilde{\mathbf{X}} \parallel^{2} \leq -\frac{\lambda_{min}(\mathbf{Q})}{2\lambda_{max}(\mathbf{P})} V(\widetilde{\mathbf{X}}) < 0.$$

By standard ISS comparison principles (Khalil, 2002; Sontag, 1989), the network trajectory is bounded for all $t \geq 0$, and the system state enters and remains trapped within the compact invariant ball B_{δ} as $t \to \infty$. This rigorously proves that systemic capital depletion and fire-sale price collapses cannot experience unbounded cascades under UCRF governance.

5. Simulation Framework and Empirical Results

To empirically validate the theoretical stability guarantees established in Section 4, this section evaluates the Universal Cybernetic Risk Framework (UCRF) through large-scale non-linear Monte Carlo stress-testing across synthetic and empirical banking network topologies.

5.1 Network Calibration and Dual-Time-Scale Stress Design

Network Topology Calibration

We synthesize an interconnected interbank ecosystem comprising $N = 100$ systemically relevant financial institutions (clearing members, prime broker-dealers, and commercial banks). The interbank exposure matrix $\mathbf{W} \in \mathrm{R}^{100\times100}$ is generated via a scale-free **Barabási-Albert preferential attachment model**, exhibiting a power-law degree distribution $P(k) \sim k^{-\gamma}$ with scaling parameter $\gamma = 2.30$, precisely matching empirical findings from the European and Federal Reserve interbank lending networks (Gai & Kapadia, 2010).

Institutional balance sheets are calibrated to standard regulatory proportions:

(1) Baseline Tier-1 capital buffers $e_i(0)$ are uniformly drawn from U[8%, 14%] of risk-weighted assets.

(2) Unencumbered funding liquidity reserves $l_i(0)$ represent U[5%, 10%] of total assets.

(3) Asset portfolio overlap q_i is distributed such that systemic hubs share large common inventory

holdings, generating realistic vulnerability to fire-sale spirals.

Dual-Time-Scale Control Architecture

To resolve the temporal paradox of "instantaneous capital injections," we formalize the operational stabilization over a **dual-time-scale hierarchy**:

(1) **Fast-Scale Actuation ($\tau \in [0,2000]$ms):** Governed by automated CCP clearing rules, this inner loop actuates sub-second algorithmic order throttles, raises margin haircuts proportionally to $\mathrm{A}_i(t)$, and executes localized trading freezes when local price velocity crosses safety bounds.

(2) **Slow-Scale Actuation ($t \in [1,60]$minutes):** Governed by central bank emergency liquidity facilities (Lender of Last Resort, LOLR), this outer loop allocates scarce, budget-constrained liquidity injections $u_{l,i}(t)$ to core systemic nodes under statutory cap $B_{total} = 0.05 \sum_{i=1}^{N} e_i(0)$ (5% of aggregate initial network equity).

Extreme Stress Scenario and Benchmarking Regimes

At $t = 0$, an exogenous tail shock hits the top 5 most central network hubs simultaneously, instantly wiping out 40% of their equity buffers ($d_{e,i}(0) = -0.4e_i(0)$). We benchmark UCRF against four comparative regimes under 500 independent Monte Carlo trials:

Regime 1: Uncontrolled Baseline: Open-loop contagion with zero real-time intervention.

Regime 2: Static Capital Buffer (Basel III/IV): Institutions maintain fixed 10.5% capital buffers but execute uncoordinated, decentralized balance-sheet de-risking and asset liquidations.

Regime 3: Open-Loop Circuit Breaker: Nodes halt trading whenever asset price declines exceed a fixed 7% volatility threshold.

Regime 4: Equal-Budget Uncoordinated Bailout (Crucial Benchmark): Distributes the exact same total liquidity budget B_{total} uniformly across distressed institutions, but *without* cybernetic feedback scheduling.

Regime 5: UCRF Closed-Loop Control (Proposed): Gain-scheduled, state-feedback control satisfying the LMI conditions of Theorem 1 under identical budget constraint B_{total}.

5.2 Empirical Results and Comparative Analysis

Table 1 summarizes the cross-regime performance across key macroprudential stress metrics.

Table 1: Cross-Framework Comparative Stress Performance ($N = 100$, 500 Monte Carlo Trials)

Performance Metrics	Regime 1: Uncontrolled Baseline	Regime 2: Static Basel Buffer	Regime 3: Circuit Breaker	Regime 4: Equal-Budget Bailout	Regime 5: UCRF (Proposed)
Systemic Default Rate (%)	68.2%	41.5%	33.0%	22.8%	**6.4%**
Max Capital Drawdown (%)	58.4%	39.1%	31.7%	26.4%	**9.8%**
Amihud Illiquidity Spike (×)	14.2 ×	9.8 ×	7.1 ×	5.4 ×	1.6 ×
Inner-Loop Halting Time (ms)	∞ (Failed)	N/A	8,900ms	N/A	620ms
Outer-Loop Stabilization (min)	∞ (Failed)	42.5min	28.0min	18.4min	4.2min
Budget Consumption (B_{spent}/B_{total})	0.0%	0.0%	0.0%	100.0%	61.2%
False-Positive Intervention Rate	N/A	High	51.2%	N/A	3.9%

Note: Data reflects sample means over 500 independent Monte Carlo runs. Inner-loop halting time indicates algorithmic cascade arrest; outer-loop indicates complete return to the ISS compact invariant set B_δ.

5.3 Macroprudential Insights: Why Feedback Topology Beats Pure Liquidity Volume

A pivotal finding illustrated by Table 1 is the marked contrast between **Regime 4 (Equal-Budget Bailout)** and **Regime 5 (UCRF)**. Both regimes have access to the exact same central bank emergency reserve B_{total}. However, Regime 4 still suffers a 22.8% default rate and fully exhausts 100% of the public budget.

Because financial networks are highly asymmetric, uncoordinated liquidity distribution squanders critical public resources on peripheral nodes that pose minimal systemic contagion risk. UCRF's gain matrix $\mathbf{K}(\mathbf{X})$, parameterized by the real-time topological distress index $\Omega(t)$ and microstructure depth $A_i(t)$, acts as a **cybernetic filter**. It precisely concentrates liquidity actuation on the critical transmission bottlenecks of the network graph, quenching the contagion cascade before secondary fire-sale feedback loops can ignite.

6. Implementation Challenges and Limitations

While the Universal Cybernetic Risk Framework (UCRF) provides rigorous, analytically verified stability guarantees under ideal state feedback, its translation into operational central banking architectures and Central Counterparty Clearinghouse (CCP) risk engines faces five non-trivial engineering and institutional constraints.

6.1 Control-Theoretic and Operational Engineering Challenges

6.1.1 Incomplete State Observability and the Need for Dynamic Observers

A primary theoretical assumption of pure state feedback ($\mathbf{u} = -\mathbf{K}\widetilde{\mathbf{X}}$) is full, instantaneous observability of the complete network state $\mathbf{X}(t) \in \mathrm{R}^{3N}$. In practice, while core marketable asset prices $\mathbf{p}(t)$ and centralized CCP clearing margins are observable at sub-second frequencies, bilateral Over-the-Counter (OTC) derivative exposures and unencumbered funding liquidity reserves $\mathbf{l}(t)$ are notoriously opaque and reported with significant reporting delays.

Mitigation Pathway: Operational deployment requires augmenting UCRF with an **Extended Kalman Filter (EKF)** or a high-gain **Luenberger-type dynamic state observer**:

$$\frac{d\widehat{\mathbf{X}}(t)}{dt} = \mathbf{A}\widehat{\mathbf{X}}(t) + \mathbf{B}\mathbf{u}(t) - \mathbf{B}_{\Phi}\mathbf{\Phi}(\hat{\boldsymbol{e}}(\mathbf{t}))+\mathbf{L}(\mathbf{y}(\mathbf{t})-\boldsymbol{C_{obs}}\widehat{\mathbf{X}}(t)), \quad (\mathbf{14})$$

where $\mathbf{y}(t)$ denotes the vector of partially observed market prices, repo spreads, and CCP variation margins, and $\mathbf{L}$ is the observer gain matrix. Regulators must guarantee that the coupled controller-observer system satisfies the classical Separation Principle under sector-bounded non-linearities.

Furthermore, state observer matrices can be integrated with contemporary machine-learning-driven balance-sheet forecasting methodologies (e.g., Do, 2025), which predict non-linear drifts in firm-level operational performance and return dynamics, thereby refining the baseline drift estimates within the Extended Kalman Filter.

6.1.2 Actuator Saturation and Integrator Windup under Extreme Tail Crises

As formalized in Section 3.3, real-world stabilization is strictly bounded by statutory rescue capacities $\sum(u_{e,i} + u_{l,i}) \leq B_{total}$. When an unprecedented macro-shock exceeds the critical threshold ($d_{max} > d_{crit}$), the commanded control $\mathbf{u}_{cmd}(t)$ hits physical saturation boundaries ($\mathbf{u} = \mathbf{U}_{max}$).

Engineering Risk: Under sustained saturation, the discrepancy between commanded and realized actuation induces severe **integrator windup**. If the gain-scheduling matrix $\mathbf{K}(\mathbf{X})$ excessively accumulates past tracking errors during prolonged crises, the controller will experience catastrophic lag when attempting to withdraw intervention during market recovery, causing destabilizing secondary liquidity overshoots.

Mitigation Pathway: The implementation of **anti-windup compensation loops** and dynamic dead-zone limiters is mathematically mandatory to guarantee local stability when the system operates at statutory capacity frontiers.

6.1.3 High-Frequency Control Chattering and Limit Cycles

The inner-loop fast actuation (sub-second margin adjustments and algorithmic order throttling) introduces

discontinuous switching dynamics. If market volatility hovers precisely around circuit-breaker trigger thresholds, the interaction between microsecond execution algorithms and continuous-time feedback can generate **chattering (high-frequency limit cycles)**. This artificial oscillation risks injecting synthetic microstructure noise into order books, unintentionally widening bid-ask spreads. *Mitigation Pathway:* Replacing discontinuous step triggers with smooth, sigmoid-regularized boundary layer approximations ($tanh\,(\cdot)$ or saturation smoothers) guarantees smooth state trajectories while preserving Lyapunov dissipation.

6.2 Economic, Game-Theoretic, and Regulatory Frictions

6.2.1 Endogenous Moral Hazard and Strategic Free-Riding

The existence of a provably stabilizing cybernetic backstop fundamentally alters the microeconomic risk incentives of market participants. Empirical research on banking behavior demonstrates that extraordinary central bank monetary policy interventions and emergency liquidity accommodations significantly amplify institutional risk-taking channels during periods of severe macroeconomic uncertainty (Idun et al., 2025). If commercial banks and prime broker-dealers possess perfect knowledge that UCRF strictly confines network drawdowns to a compact invariant set B_{δ}, they face an acute moral hazard incentive: institutions will rationally increase asset leverage and minimize private, costly liquidity cushions $l_i(t)$, anticipating that the central bank's cybernetic controller will socialize extreme tail losses.

Policy Mechanism Design: To counteract strategic free-riding, UCRF must be paired with **ex-post Pigouvian cybernetic insurance levies**. Institutions should be assessed dynamic supervisory fees proportional to the cumulative control energy they consume during stress periods:

$$\mathcal{F}_i = \int_0^T \big(\mathbf{u}_i(t)^T \boldsymbol{R}_i \mathbf{u}_i(t)\big) dt\,. \tag{15}$$

By internalizing the social cost of systemic stabilization, institutions are economically disincentivized from exploiting the cybernetic safety net.

6.2.2 Cross-Border Jurisdictional Asynchrony and Information Latency

Modern financial networks operate across fragmented legal boundaries and multi-currency payment rails (e.g., Fedwire, TARGET2, CHAPS). In cross-border contagion scenarios, information exchange and emergency repo authorizations encounter heterogeneous legal protocols and latency lags ($\tau_d \in [100\text{ms}, 5\text{s}]$).

Theoretical Implication: Network dynamics with discrete or distributed communication delays must be modeled as functional differential equations:

$$\frac{d\widetilde{\mathbf{X}}(t)}{dt} = \mathbf{A}\widetilde{\mathbf{X}}(t) + \mathbf{B}\mathbf{u}(t-\tau_d) - \mathbf{B}_{\Phi}\boldsymbol{\Phi}\big(\tilde{\mathbf{e}}(t-\tau_d)\big) + \mathbf{D}\mathbf{d}(t). \tag{16}$$

If information latency τ_d exceeds the critical phase margin of the open-loop network, feedback actuation will arrive out-of-phase, transforming stabilizing damping forces into destabilizing shock amplifiers (feedback-induced hunting). Deploying UCRF across international borders therefore requires synthesizing **delay-dependent Lyapunov-Krasovskii functionals** to establish the maximum permissible latency upper bound τ_{max} under which stability is preserved.

7. Conclusion

This paper has established the **Universal Cybernetic Risk Framework (UCRF)** as a mathematically rigorous, closed-loop stabilization paradigm for mitigating systemic risk in hyper-connected financial networks. Traditional macroprudential monitoring architectures—governed by static capital adequacy directives (Basel III/IV) and passive, backward-looking statistical indicators (VaR, Expected Shortfall, and static clearing vectors)—suffer from structural phase-lag vulnerabilities during rapid non-equilibrium liquidation events. By reconceptualizing systemic financial infrastructure through the lens of modern non-linear control engineering, UCRF transforms systemic risk mitigation from an open-loop observational diagnostic into an active, automated state-feedback stabilization architecture tailored for Central Counterparty Clearinghouses (CCPs) and central bank emergency lending facilities.

Theoretical and Methodological Advances

The methodological architecture of UCRF resolves several persistent theoretical bottlenecks in quantitative systemic risk literature:

(1) **Coupled High-Dimensional Dynamics:** We formulated a unified $3N$-dimensional continuous-time state-space representation that reconciles direct balance-sheet insolvency contagion with indirect, microstructure-mediated fire-sale spirals and funding liquidity runs.

(2) **Lur'e System Formulation and Absolute Stability:** By framing piecewise-linear counterparty default thresholds as sector-bounded non-linearities, we mapped the multi-asset banking network into an interconnected Lur'e dynamical system. Utilizing Lur'e-Postnikov Lyapunov candidate functions and the S-procedure, we reduced the global asymptotic stabilization problem to a set of computationally tractable, convex Linear Matrix Inequalities (LMIs).

(3) **Input-to-State Stability (ISS) Guarantees:** We provided rigorous mathematical proofs that under bounded exogenous macroeconomic stress shocks, the closed-loop financial network satisfies strict ISS criteria. We analytically derived the explicit boundary layer of the compact invariant attractor set B_{δ}, establishing that systemic drawdowns are provably bounded against worst-case tail distributions.

(4) **Economic Resource Realism:** Departing from unconstrained "infinite bailout" abstractions, UCRF formally embeds component-wise actuator saturation and statutory central bank liquidity budget ceilings (B_{total}), transforming the intervention law into a realistic constrained optimal allocation

problem.

Empirical and Macroprudential Policy Implications

Extensive Monte Carlo stress-testing on scale-free interbank networks under a **dual-time-scale hierarchy** (sub-second algorithmic margin and order-throttling inner loops paired with multi-minute liquidity facility outer loops) validates the operational superiority of UCRF. Crucially, when compared against an **Equal-Budget Uncoordinated Bailout** baseline consuming the exact same fiscal envelope, UCRF reduces the systemic node failure rate from 22.8% to 6.4%, caps peak network capital drawdowns at 9.8%, and consumes only 61.2% of the emergency public reserve. This demonstrates empirically that **cybernetic feedback scheduling—targeting dynamic network bottlenecks via real-time topological indices** $\Omega(t)$ **and market illiquidity** $\mathrm{A}_i(t)$**—is substantially more potent than the uncoordinated injection of raw capital volume**.

Avenues for Future Research

While UCRF establishes a solid mathematical foundation, several promising frontiers warrant future exploration:

- **Decentralized Dynamic Observers:** Developing distributed Extended Kalman Filters (EKFs) or H_∞ observers to dynamically reconstruct unobservable OTC bilateral exposures under strategic reporting concealment.
- **Delay-Dependent Compensation:** Incorporating Lyapunov-Krasovskii functionals to establish analytical stability bounds in cross-border settlement environments subject to variable communication latencies.
- **Data-Driven Adaptive Synthesis:** Integrating deep reinforcement learning and Model Predictive Control (MPC) to adaptively synthesize time-varying gain schedules $\mathbf{K}(\mathbf{X})$ under dynamically mutating network topologies.

In conclusion, UCRF provides central banks, sovereign wealth entities, and systemic clearinghouses with a quantifiable, mathematically verified, and computationally executable blueprint to safeguard global multi-trillion-dollar financial ecosystems against catastrophic cascading collapse.

References

Amihud, Y. (2002). Illiquidity and stock returns: Cross-section and time-series effects. *Journal of Financial Markets, 5*(1), 31–56. https://doi.org/10.1016/S1386-4181(01)00024-6

Ashby, W. R. (1956). *An introduction to cybernetics*. John Wiley & Sons. https://doi.org/10.5962/bhl.title.5851

Battiston, S., Puliga, M., Kaushik, R., Tasca, P., & Caldarelli, G. (2012). DebtRank: Too central to fail? Financial networks, the FED and systemic risk. *Scientific Reports, 2*, Article 541. https://doi.org/10.1038/srep00541

Boyd, S., El Ghaoui, L., Feron, E., & Balakrishnan, V. (1994). *Linear matrix inequalities in system and control theory*. Society for Industrial and Applied Mathematics. https://doi.org/10.1137/1.9781611970777

Brunnermeier, M. K., & Pedersen, L. H. (2009). Market liquidity and funding liquidity. *The Review of Financial Studies, 22*(6), 2201–2238. https://doi.org/10.1093/rfs/hhn098

Chan, L., & Wong, W. K. (2012). Automated trading with genetic-algorithm neural-network risk cybernetics: An application on FX Markets. *Finamatrix Journal, February*.

Chan, L., & Wong, W. K. (2018). Fix Risk-Cybernetics Protocol. *Available at SSRN 3111877*.

Cifuentes, R., Ferrucci, G., & Shin, H. S. (2005). Liquidity risk and contagion. *Journal of the European Economic Association, 3*(2–3), 556–566. https://doi.org/10.1162/jeea.2005.3.2-3.556

Cont, R., & Schaanning, E. (2017). Fire sales, indirect contagion and systemic stress testing (Working Paper No. 2/2017). Norges Bank. https://doi.org/10.2139/ssrn.2541114

Do, Q. H. (2025). Forecasting ROA and ROE for Retail Companies in Vietnam by Using Machine Learning Techniques. *Advances in Decision Sciences*, *29*(4), 1-30.

Eisenberg, L., & Noe, T. H. (2001). Systemic risk in financial systems. *Management Science, 47*(2), 236–249. https://doi.org/10.1287/mnsc.47.2.236.9835

Gai, P., & Kapadia, S. (2010). Contagion in financial networks. *Proceedings of the Royal Society A: Mathematical, Physical and Engineering Sciences, 466*(2120), 2401–2423. https://doi.org/10.1098/rspa.2009.0410

Greenwood, R., Landier, A., & Thesmar, D. (2015). Vulnerable banks. *Journal of Financial Economics, 115*(3), 471–485. https://doi.org/10.1016/j.jfineco.2014.11.006

Hansen, L. P., & Sargent, T. J. (2008). *Robustness*. Princeton University Press.

Huang, C., Miao, H., Yang, X., Cao, J., & Yang, H. (2025). Cascading failure, financial network and systemic risk. *The North American Journal of Economics and Finance, 80*, Article 102505. https://doi.org/10.1016/j.najef.2025.102505

Idun, A. A. A., Woode, J. K., & Junior, P. O. (2025). Time-varying analysis of monetary policy channels of banking system risk-taking in Ghana amidst the COVID-19 uncertainty. *Annals of Financial Economics*, *20*(01), 2550007.

Khalil, H. K. (2002). *Nonlinear systems* (3rd ed.). Prentice Hall.

Khan, H., Wong, W. K., & Yeo, S. K. (2005). Has Trade Increased the Risk of Contagion? An Empirical Investigation.

Kyle, A. S. (1985). Continuous auctions and insider trading. *Econometrica, 53*(6), 1315–1335.

https://doi.org/10.2307/1913210

Lur'e, A. I., & Postnikov, V. N. (1944). On the theory of stability of control systems. *Prikladnaya Matematika i Mekhanika*, *8*(3), 246–248. (In Russian).

Montañez Jacquez, S., Quezada Téllez, L. A., Morales Mendoza, R., Moya-Albor, E., Fernández Anaya, G., & Santos Moreno, M. (2026). Critical regimes of systemic risk: Flow network cascades in the U.S. banking system. *Risks, 14*(4), Article 73. https://doi.org/10.3390/risks14040073

Sindhu, M. I., Windijarto, Wong, W. K., & Maswadi, L. (2026). Unveiling hidden connectedness between cryptocurrency and stock markets in BRICS: a TVP-VAR perspective. *Kybernetes*, *55*(6), 2627-2647.

Sontag, E. D. (1989). Smooth stabilization implies coprime factorization. *IEEE Transactions on Automatic Control, 34*(4), 435–443. https://doi.org/10.1109/9.28018

Suissi, N., & Mroua, M. (2026). The Effect of the Russia–Ukraine Invasion on Macroeconomic Variables, Investor Sentiment and Commodities: A Frequency Connectedness among G7. *Annals of Financial Economics*, *21*(02), 2650006.

Wan Jr, H., & Wong, W. K. (2001). Contagion or inductance? Crisis 1997 reconsidered. *The Japanese Economic Review*, *52*(4), 372-381.

Wiener, N. (1948). *Cybernetics: Or control and communication in the animal and the machine*. MIT Press.